Effect of Dense Gas CO_2 on the Coacervation of Elastin

Fariba Dehghani,*,† Nasim Annabi,† Peter Valtchev,† Suzanne M. Mithieux,‡ Anthony S. Weiss,‡ Sergei G. Kazarian,§ and Feng H. Tay§

School of Chemical and Biomolecular Engineering, University of Sydney, Sydney, New South Wales 2006, Australia, School of Molecular and Microbial Biosciences, University of Sydney, Sydney, New South Wales 2006, Australia, and Department of Chemical Engineering, Imperial College London, South Kensington Campus, London, SW7 2AZ, United Kingdom

Received August 10, 2007; Revised Manuscript Received October 3, 2007

In this study for the first time the effect of high-pressure CO_2 on the coacervation of α-elastin was investigated using analytical techniques including light spectroscopy and attenuated total reflection Fourier transform infrared (ATR-FTIR) spectroscopic imaging and circular dichroism (CD) spectroscopy. The coacervation behavior of α-elastin, a protein biopolymer, was determined at temperatures below 40 °C and pressures lower than 180 bar. At these conditions elevated pressures did not disrupt the ability of α-elastin to coacervate. It was feasible to monitor the presence of amide I, II, and III bands for α-elastin at high-pressure CO_2 using ATR-FTIR imaging. At a constant temperature the peak absorption was substantially enhanced by increasing the pressure of the system. CD analysis demonstrated the preservation of secondary structure attributes of α-elastin exposed to dense gas CO_2 at the pressure range investigated in this study. The lower critical solution temperature of α-elastin was dramatically decreased from 37 to 16 °C when the CO_2 pressure increased from 1 to 50 bar, without a significant change after that. Carbon dioxide at high pressures also impeded the reversible coacervation of α-elastin solution. These effects were predominantly associated with the lowered pH of the aqueous solution and maybe the interaction between CO_2 and hydrophobic domains of α-elastin.

Downloaded via UNIV OF CALIFORNIA LOS ANGELES on January 17, 2025 at 21:58:47 (UTC).
See https://pubs.acs.org/sharingguidelines for options on how to legitimately share published articles.

Introduction

Protein stability can be represented by a two-dimensional pressure−temperature ($P-T$) diagram.[1] Thermal denaturation, which has been studied widely, is a one-dimensional section of the $P-T$ diagram.[1] Bridgman observed that egg white albumin is denatured at 7000 bar with effects similar to but not identical with temperature denaturation.[2] The effects of pressure on proteins precede temperature effects as the pressure changes the distances between constituents and affects the internal interactions, but the total energy content of the system remains stable. However, both volume and energy content of the system are changed by increasing the temperature.[3] Pressure affects the partial molar volume of a protein, its folding properties, and conformation. These effects can be elastic (reversible) or plastic (irreversible).[1,4] An elastic effect can occur at pressures below 5000 bar with preservation of protein secondary structure.[1,4] Pressure may change the length of chemical bonds and hydration state and diminish cavity sizes in a protein molecule but does not alter its molecular folding.[1] Plastic effects usually occur at pressures above 5000 bar, which results in rotational changes around backbones and secondary structure of a protein.[1,4] Protein–protein interactions and protein–ligand binding can be affected at lower pressures.[5]

There has been remarkable progress in the application of dense gases (DGs) to the processing of polymers over the past decade.[6] Dense gases are those that are near or above their critical point, generally with a reduced temperature (T/T_c) and pressure (P/P_c) between 0.9 and 1.2. Beyond the critical point, the substance is called a supercritical fluid and has solvation strength approaching that of liquids and diffusivity approaching that of gases. DG technology has been used for processing polymers including synthesis, fractionation, impregnation, and fabrication of polymeric scaffolds.[7,8]

The most commonly used DG is carbon dioxide because it has low critical parameters ($T_c = 31.1$ °C, $P_c = 73.8$ bar), is inexpensive, and is nontoxic. Carbon dioxide is also particularly useful for biomaterial processing because its critical temperature is close to ambient temperature. Carbon dioxide is relatively miscible with a variety of organic solvents and is easily recovered after processing due to its high volatility at atmospheric conditions. Therefore it is easy to remove, resulting in the production of product with no residual solvent.

High-pressure CO_2 has been used as a volatile acid for the isoelectric precipitation of proteins.[9,10] Using a volatile electrolyte for proteins precipitation is a valuable tool as it can be used as a substitute for mineral acids such as sulfuric acid and hydrochloric acid commonly used in conventional processes.[9] Protein denaturation due to extreme decrease in pH in conventional processes can be eliminated as the acid concentration can be controlled by pressure, using a volatile acid.[9]

The objective of this study was to investigate the effect of DG CO_2 on the reversible molecular association of protein biopolymers. Elastin, the major component of elastic fibers, is an insoluble extracellular matrix protein found in skin, bladder, lung, ligament, elastic cartilage, and arteries.[11] It provides elasticity and resilience to maintain the proper function of tissues that are subjected to repetitive distension and physical stress.[12–14] Elastin is the most persistent protein in the body. It is particularly established by assembly of its precursor tropoelastin in utero.[15] Elastin is an extremely insoluble biopolymer and is difficult to process into new biomaterials, so α-elastin, an oxalic acid

* To whom the correspondence should be addressed: e-mail: F.Dehghani@usyd.edu.au; telephone: (++612) 93514794; fax: (++612) 93512854.
† School of Chemical and Biomolecular Engineering, University of Sydney.
‡ School of Molecular and Microbial Biosciences, University of Sydney.
§ Department of Chemical Engineering, Imperial College London.

10.1021/bm700891b CCC: $40.75 © 2008 American Chemical Society
Published on Web 03/26/2008

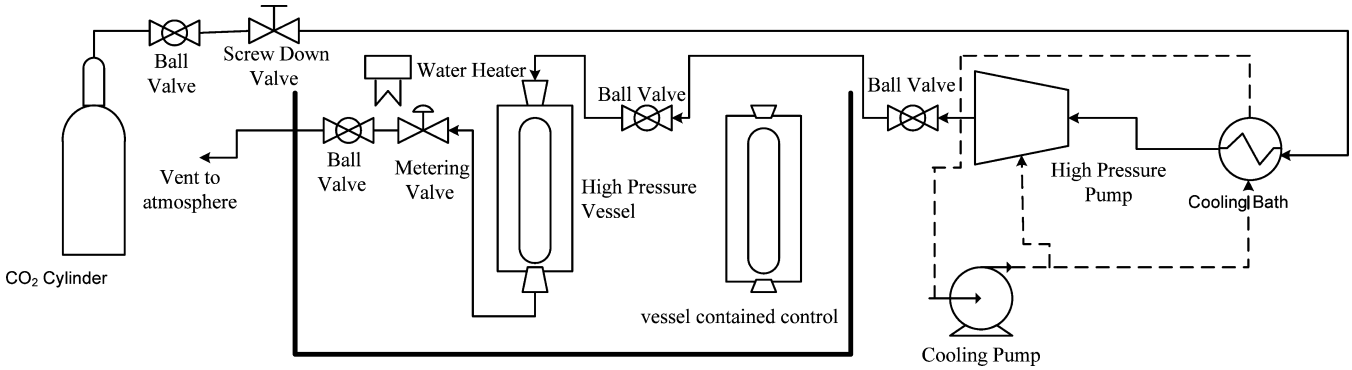

Figure 1. Experimental setup used for high-pressure experiments.

solubilized derivation of elastin, is frequently used for synthesizing elastin-based materials[16] as it undergoes reversible self-association.[17] At low temperature both tropoelastin[12,13,18] and α-elastin[17] are soluble in aqueous buffers, while at about physiological temperature a phase separation or coacervation occurs. Coacervation plays a crucial role during elastin formation by concentrating and aligning monomers prior to cross-linking[12,13] to form fibers.[17,18] Coacervation of these soluble molecules is a concentration-dependent process and can be interpreted as an intermolecular hydrophobic association[13,17] where solution variables such as biopolymer concentration, pH, salt, and impurities can influence its efficacy.[12,13,19,20]

Recent advances in design of high-pressure vessels for in situ analysis allow for studies of the effects of pressure on protein folding and association by fluorescence spectroscopy, Raman spectroscopy, nuclear magnetic resonance (NMR), and Fourier transform infrared spectroscopy (FTIR).[1] Circular dichroism (CD) can detect pressure-induced changes in proteins after depressurization but not during the pressure treatment as the coupling of high pressure to CD presents unsolved technical obstacles.[1] Therefore, CD analysis can be used to examine the consequences of pressure exposure when these changes are largely irreversible.[1] FTIR can be used at high pressures[1–5] where the amide I C═O stretching coupled with CN stretching and CCN deformation provides information on secondary structure which can be determined using the second derivative and Fourier self-deconvolution.[1]

The recent development of attenuated total reflection Fourier transform infrared (ATR-FTIR) spectroscopic imaging using a diamond accessory permits in situ study of various systems exposed to high-pressure CO_2. This approach was used to study CO_2-induced phase separation in polymer blends[21] and polymer interdiffusion[22] under high-pressure CO_2. In this paper, the feasibility of utilizing ATR-FTIR spectroscopic imaging applied to aqueous solutions at high pressures was assessed to investigate the molecular aggregation of α-elastin. This is the first time that ATR-FTIR technique was used for characterization of protein secondary structure at high pressures. The effects of pH, salt, and α-elastin concentrations on the coacervation behavior of α-elastin were defined at atmospheric and high pressures.

Materials and Methods

Materials. α-Elastin (molecular weight ≈ 60000) extracted from bovine ligament was purchased from Elastin Products Co. (Owensville, MO). Carbon dioxide (99.99% purity) and high-purity nitrogen were supplied by BOC (Murray Hill, NJ). All aqueous solutions were prepared in MilliQ water. α-Elastin was dissolved in PBS (phosphate-buffered saline; 10 mM sodium phosphate pH 7.4, 1.35 M NaCl) at 5 mg/mL, and the solution was dissolved overnight at 4 °C prior to use.

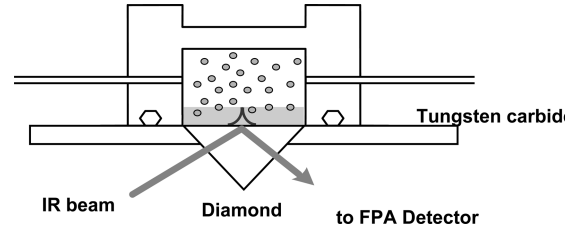

Figure 2. Schematic diagram of the high-pressure cell combined with ATR accessory.

Effect of Pressure on α-Elastin. The schematic diagram of the apparatus used for investigating the effect of CO_2 pressure on α-elastin is shown in Figure 1. A high-pressure pump (Thar, model P50) was used to transfer CO_2 into the high-pressure view cell (Jerguson sight gauge, model R32). A recirculation heater (Ratek) was used to control the temperature of the water bath, and the pressure of the system was monitored using a pressure transducer (Druck).

In each experiment 2 mL of a fresh solution of α-elastin, which was prepared overnight, was injected into a glass tube located inside the high-pressure vessel. No coacervation was observed for the 5 mg/mL α-elastin used in this study at temperatures below 32 °C and atmospheric pressure. After thermal equilibrium was established in the system, the air was purged using an inert gas (e.g., CO_2) at 5 bar pressure. The system was then pressurized with the DG CO_2 to different pressures ranging from 5 to 180 bar. While the pressure was kept constant, the temperature was increased incrementally from 7 to 37 °C. The temperature at which the solution became turbid was monitored. The reversibility of coacervation behavior was visually verified upon decreasing the temperature while the pressure was kept constant. The system was then depressurized slowly to minimize foaming, and the sample was collected. In addition, a sample of α-elastin solution was also placed in the water bath at atmospheric pressure, as a control, and its coacervation behavior was monitored upon increasing the temperature.

Spectrophotometry. A 5 mg/mL α-elastin solution in PBS was prepared. Control and pressurized α-elastin solutions were monitored by spectrophotometry (Varian, Cary 3) after depressurization over a range of temperatures. Coacervation was monitored at 300 nm where the cuvette holder was connected to a recirculating water bath to control the temperature. At each temperature, turbidity was measured for 5 min. Following each analysis, the solutions were cooled to return turbidity to the baseline.

Attenuated Total Reflection Fourier Transform Infrared Spectroscopic Imaging (ATR-FTIR). The high-pressure cell used in this experiment is similar to that used by Kazarian and Chan.[21] The schematic diagram of the apparatus used in this study is shown in Figure 2. The high-pressure cell was sealed with a poly(tetrafluoroethylene) (PTFE) spacer against the tungsten carbide disk, and force was exerted by using the arm of the ATR accessory to lock the cell in position. The temperature in the high-pressure cell can be adjusted using the temperature control unit connected to the top plate of the ATR accessory. Once thermal equilibrium was reached, the cell was slowly

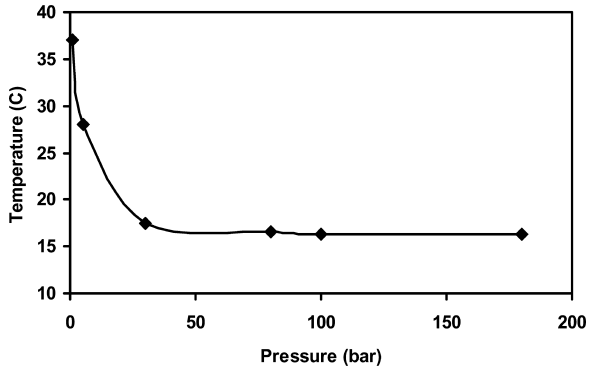

Figure 3. The effect of pressure on coacervation temperature.

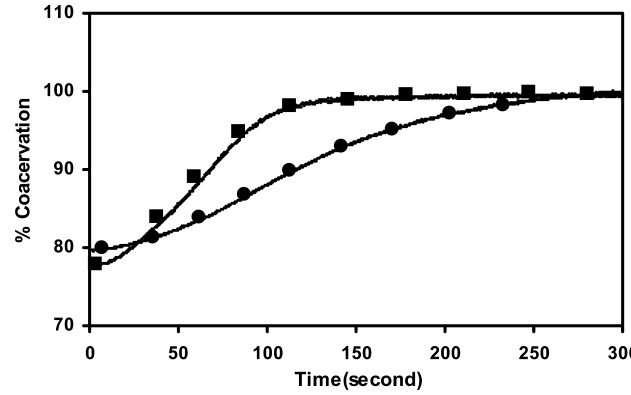

Figure 4. The effect of CO_2 pressure on the coacervation of α-elastin at 37 °C: control (■); 180 bar(●).

loaded with CO_2 using an ISCO model 500D syringe pump. The pressure of the system was monitored during the pressurization stage and throughout the course of the experiment using a digital pressure transducer.

The FTIR images were obtained with the setup described elsewhere[23] using a diamond ATR accessory (Specac, Ltd.) and a 64 × 64 focal plane array detector.[21–24] The imaging ATR spectrometer has been patented by Varian, Inc.[25] The diamond ATR-FTIR accessory was positioned in the macrochamber and carefully aligned prior to the measurement. The sample area measured by this macro-ATR imaging approach is ca. 500 × 700 μm.[2] The spatial resolution in micro-ATR-FTIR imaging using a Ge crystal is ca. 3–4 μm, while spatial resolution in macro-ATR FTIR imaging using a diamond accessory is ca. 15 μm.[23] No subtraction was done to the spectra. This is usually not required in the case of ATR-FTIR spectroscopy.

Imaging spectra were collected with 32 coaddition, a spectral range of 3950–900 cm^{-1}, and a spectral resolution of 4 cm^{-1}. Scanning time for each image was approximately 40 s. The FTIR images of the 20 mg/mL α-elastin sample at different pressures and temperatures were collected, and the effect of pressure on the secondary structure of protein was studied. At lower concentrations, no significant absorption of amide peaks corresponded to α-elastin was observed by ATR-FTIR spectroscopic imaging at atmospheric and high pressures. The solution of 20 mg/mL was coacervated at 20 °C and atmospheric pressure.

Circular Dichroism (CD) Spectroscopy. Circular dichroism analyses for control and α-elastin solutions exposed to 150 bar CO_2 were carried out in a 0.1 mm path length cuvette at 20 °C using a Jasco J-720 spectropolarimeter over 180–260 nm with 12 spectral accumulations. Data were expressed in terms of the mean residue ellipticity in units of deg cm^2 $dmol^{-1}$. Secondary structure calculations were obtained using CDPro.[26]

Results and Discussions

The effect of CO_2 on coacervation of α-elastin was determined at various pressures and temperatures ranging from 1 to 180 bar and 7 to 37 °C. Carbon dioxide exhibited a profound effect on the coacervation temperature of α-elastin. The temperature at which coacervation commenced was substantially diminished as the CO_2 pressure increased (Figure 3). The coacervation temperature decreased from 37 to 16 °C when the pressure was increased from 1 to 50 bar and above this pressure approached a plateau. The reversible coacervation behavior at atmospheric pressure was rapid and commonly took place in less than 1 min. However, samples pressurized with CO_2 at above 30 bar required at least 45 min to achieve partial solubilization after coacervation and decreasing the temperature to 7 °C. The solution was not completely clear as control sample after it was kept under 30 bar for 4 h at 7 °C. However, it was converted to a very clear solution upon depressurization of the sample to pressures below 10 bar. The CO_2 pressure therefore altered the rapid reversible coacervation that is seen at atmospheric pressure when the temperature of the solution is decreased from 37 to 20 °C.

Spectrophotometry. The coacervation behavior of α-elastin solutions exposed to CO_2 at various pressures was monitored by UV spectrophotometry after depressurization and compared with control samples (Figure 4). At pressures above 60 bar, CO_2 affected the coacervation profiles of α-elastin solutions. While the control sample approached 100% coacervation within 114 s, samples exposed to CO_2 at pressures above 60 bar achieved this within 214 s. The retardation was more profound for samples exposed to higher pressures, even though the pH of all solutions after depressurization were similar to untreated sample. The effect of pressure on the reversible coacervation profile of α-elastin exposed to nitrogen at 180 bar and CO_2 at pressures below 60 bar was negligible (Table 1).

The coacervation temperature of α-elastin is governed by various factors including pH, ionic strength, and protein concentration.[12,13,19,20,27] The coacervation temperature of tropoelastin[12,13] and α-elastin[27] decreased as the ionic strength increased. The influence of pH on coacervation temperature of α-elastin dissolved in pure water,[19] in buffer solution with high and low ionic strength,[27] and tropoelastin solution at PBS (150 mM NaCl)[13] were studied. At pH around the isoelectric point of α-elastin (i.e., pH = 4.8) the highest level of absorption and the lowest coacervation temperature were observed.[19] As the pH shifted from the isoelectric point, the coacervation temperature increased and the rate of turbidity decreased.[19] Coacervation was prevented at pH values far from the isoelectric point of α-elastin at below 3 or above 8.[19] A minimum in coacervation temperature of α-elastin at pH 5.3 was also observed by Partridge et al. when a solution with an ionic strength of 0.01 was used.[27] However, the concave upward profile in temperature versus pH diagram of α-elastin was not observed for solutions with high ionic strength such as 0.1; the coacervation temperature was decreased by lowering the pH of the protein solution.[27] Vrhovski et al. reported that the coacervation of tropoelastin dissolved in PBS (150 mM NaCl) decreased from 42 to 36 °C as the pH increased.[13]

The effect of DG CO_2 on coacervation temperature and partially reversible coacervation of α-elastin solution may be due to the lower free energy of the hydrophobic core of the coacervate, compared with the usual conformation, which then achieved a folded state. The reverse transition is, therefore, no longer thermodynamically favorable, and the newly formed coacervate might have a higher stability. The main contributing factor to this transition and exact mechanism of action is currently unknown. The reduction in the coacervation temper-

Table 1. Effect of CO_2 Pressure on the Time to Achieve Maximum Coacervation for α-Elastin

	1 bar	5 bar	30 bar	60 bar	80 bar	100 bar	180 bar	180 bar[a]
time for 100% coacervation (s)	114	114	114	164	211	229	252	114
pH (after depressurization)	6.3	6.2	5.9	6.1	6	5.9	6.2	6.1

[a] Nitrogen was used in this experiment.

ature of α-elastin solution in DG CO_2 system may be due to a decrease in the pH of the protein solution caused by dissolved CO_2 with a potential contribution by a depression of the melting temperature of the hydrophobic core caused by the pressure. Each of these factors has the potential to lower the activation energy of the transition by inhibiting unfavorable side chain interactions that form spontaneously during the folding process and present distinctive energy barriers that have to be overcome in order to achieve a functional final set of conformations.

The effect of pressure alone on α-elastin coacervation was assessed by using the inert gas nitrogen at 180 bar. High-pressure nitrogen had no adverse effect on the coacervation profile of α-elastin which was reversible and rapid. Therefore, the partially reversible coacervation and decrease in coacervation temperature of α-elastin at high pressure can be due to a decrease in the pH of the protein solution caused by dissolved CO_2. The pH of the α-elastin solutions used in this study was decreased from 6 to 3 when the CO_2 pressure increased from 1 to 50 bar, which was comparable with previous studies on decreasing the pH of water under high-pressure CO_2.[9,10] As expected for a reversible system, after depressurization the solution returned to a pH close to that of the original sample as illustrated in Table 1.

High-pressure CO_2 is volatile and can dissolve in aqueous solutions to decrease the pH due to the acidification of aqueous solution and production of carbonic acid.[9,10,28] As the solubility of CO_2 in water is a function of temperature and pressure, the drop in pH of the solution will be temperature and pressure dependent. Otake and Hofland found that the pH of aqueous solution decreased dramatically when the CO_2 pressure increased.[9,28] Otake et al. observed that the pH of water decreased from 7 to 4.5 at 60 °C and 200 bar CO_2 pressure.[28] Hofland et al. also measured the pH of the aqueous solution at various pressures of CO_2. They found that the pH of pure water decreased to 3.1 at 55 bar CO_2 pressure and 25 °C.[9] At pressures below 30 bar, the pH was dramatically decreased by increasing the pressure, while at higher pressures the changes approached a plateau.[9] A decrease in pH of the α-elastin solutions exposed to CO_2 may lead to a decrease in coacervation temperature of α-elastin.

The effect of pH on coacervation temperature of α-elastin solution used in this study was investigated at atmospheric pressure. It was found that the coacervation temperature decreased from 37 to 16 °C as the pH lowered from 6 to 3.7. The data acquired were compared with results of Partridge et al. who studied the effect of ionic strength and pH on coacervation temperature of α-elastin.[27] Partridge et al. reported that the coacervation temperature of α-elastin was a function of ionic strength and pH. Increasing the ionic strength of α-elastin solution decreased the coacervation temperature.[27] The coacervation temperature of solution at ionic strength of 0.1 was 25 °C at pH 3.7.[27] The lower coacervation temperature at pH 3.7, in our study, was due to utilizing a solution with a higher ionic strength (1.3), which is almost 10-fold higher than the solution used by Partridge et al. No significant retardation was observed for coacervation behavior of α-elastin solution at pH 3.7 at atmospheric pressure as the solution coacervated rapidly at lower temperature. However, the rapid reversible coacervation was not observed for this solution by decreasing the temperature to 4 °C. The solution became partially clear after 25 min at 4 °C. The partial reversible coacervation of α-elastin in the DG CO_2 system may result from both the pH drop in the system caused by dissolved CO_2 and the interaction between the CO_2 and α-elastin while the retardation in the coacervation profile of α-elastin solution exposed to CO_2 may be associated with the interaction between CO_2 and α-elastin that may take longer time to approach the initial condition.

ATR-FTIR Spectroscopic Imaging. We constructed a novel system to characterize coacervation using ATR-FTIR spectroscopic imaging at atmospheric and high-pressure CO_2. FTIR images of α-elastin (20 mg/mL) under high-pressure CO_2 were obtained, and the distributions of amide II at different pressures are shown in Figure 5a. The images are of the same scale, and the color denotes the absorbance of the assigned spectral peak which is proportional to the concentration of amide II. As the pressure increases, a higher concentration of Amide II was detected on the ATR diamond. Spectra extracted at position X of the diamond are shown in Figure 5b. Three main peaks at 1250, 1540, and 1640 cm^{-1} corresponded to amide III, amide II, amide I, respectively. However, at lower concentrations of α-elastin (5 mg/mL), these peaks were not detected in the spectrum. Infrared spectra of α-elastin exhibited the amide I and II bands at 1655 and 1537 cm^{-1}, respectively.[29] Similar results were obtained from FTIR analysis on bovine elastin and κ-elastin,[30] human elastin,[31] bovine tropoelastin,[32] and two elastin-like poly(pentapeptides).[33] Hence, the position of observed peaks is comparable with the data in the literature at atmospheric pressure. The presence of these three peaks confirmed the secondary structure of α-elastin at temperatures above 25 °C in Figure 5b. With increase of the pressure, the amount of precipitation (i.e., elastin coacervation) on the surface of the diamond cell was increased and subsequently the absorption at each wavenumber corresponding to amide band was enhanced. The broad peak at 3700−2900 cm^{-1}, assigned to the OH stretch of water molecule, has lower absorption with increasing pressure (Figure 5c). This is a result of α-elastin molecules displacing the water molecules from the surface of the diamond cell due to increasing pressure. It can be seen that there was no shift in amides' band (i.e., amide I (1640 cm^{-1}), amide II (1540 cm^{-1}), and amide III (1250 cm^{-1})) by increasing the pressure from 1 to 80 bar. The results demonstrate that under high-pressure CO_2, even though the coacervation temperature of α-elastin diminished, the secondary structure was maintained.

Circular Dichroism. One of the objectives of this study was to confirm that the elastin conformation is preserved after exposed to carbon dioxide at high pressures. Circular dichroism was conducted immediately after depressurization of the sample exposed to CO_2 at 150 bar and 37 °C. A low concentration of α-elastin was used to avoid coacervation. The spectra of 0.1 mg/mL α-elastin exposed to CO_2 and control at 20 °C were compared (Figure 6). The CD spectra of control and α-elastin exposed to CO_2 were characterized by an intense negative band between −6000 and −8000 deg cm^2 $dmol^{-1}$ at 200 nm, indicative of a large proportion of disorder in the polypeptides.

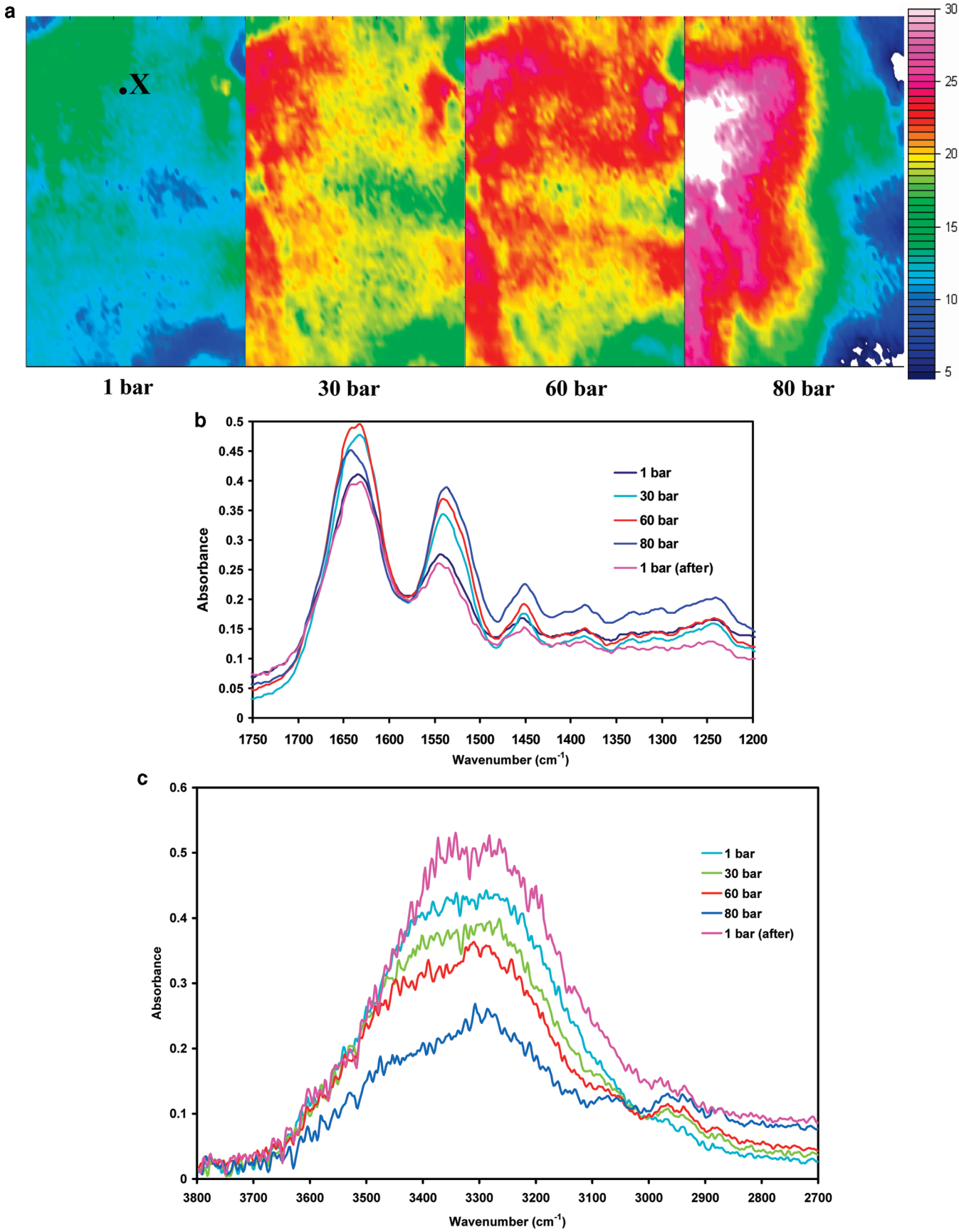

Figure 5. (a) FTIR images showing the distribution of the absorbance of the amide II band (1565−1500 cm^{-1}) at different pressures and constant temperature of 25 °C. Spectra at position denoted by X are extracted and shown in parts b and c. (b) Spectra extracted from images at different pressures showing the amide bands of α-elastin. (c) Spectra extracted from images at different pressures showing the OH stretching of water.

The presence of a less intense band centered at 222 nm suggested the existence of α-helix structure. The CD spectrum for α-elastin at ambient pressure was similar to the CD spectrum of tropoelastin,[13,32] *κ*-elastin,[30] and α-elastin.[29,34–36] It is likely

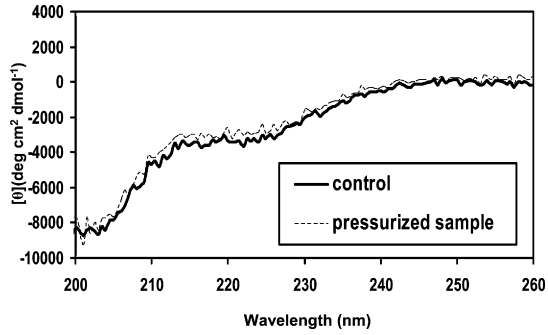

Figure 6. CD of control and α-elastin solutions exposed to CO_2 at 150 bar.

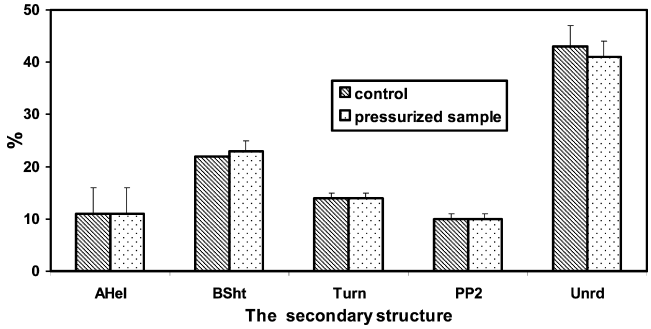

Figure 7. Effect of CO_2 pressure on the secondary structure of α-elastin.

that pressure had no persistent effect on the CD spectra of α-elastin as there was no shift for negative bands at 200 nm and the shoulder at 222 nm.

The amounts of α-helix and β-sheet were identical for both the control and the sample exposed to CO_2 (Figure 7) where the secondary structures calculated for these samples were approximately 11% α-helix, 22% β-sheet, 14% β-turn, 10% polyproline 2 turn, and 43% unresolved. The secondary structure of bovine tropoelastin was estimated to be 10% α-helix, 30% β-turn by Debelle and Alix[32] and the secondary contents of elastin to be ~10% α-helix, 35% β-strand, and 55% unresolved.[31] However, Vrhovski estimated the secondary structure of tropoelastin to be 3% α-helix, 41% β-sheet, 21% β-turn, and 33% other structures.[13] The content of α-helix of the studied protein was comparable with those of elastin[31] and bovine tropoelastin.[32]

Conclusions

CD and ATR-FTIR spectroscopic analysis confirmed that CO_2 pressure did not change the secondary structure of α-elastin. The findings presented here show it is feasible to coacervate α-elastin using CO_2 at high pressure. The present work demonstrates that high-pressure CO_2 does not disrupt the natural ability of α-elastin to coacervate but does decrease the temperature required for coacervation. High-pressure CO_2, as a volatile acid, decreased the pH of the α-elastin solution resulting in a reduction in coacervation temperature of α-elastin. Following exposure to highpressure CO_2, the α-elastin solution was also maintained in a coacervated state for a longer time. These properties may usefully provide advantages for synthesizing elastin-based biomaterials under high-pressure CO_2 as the solution can be kept in coacervated state during the reaction without using any mineral acid.

Acknowledgment. The authors acknowledge financial support from European Commission (SurfaceT project NMP2-CT-2005-013524), ARC DP0665514 and ARC DP0774289.

References and Notes

(1) Dzwolak, W.; Kato, M.; Taniguchi, Y. *Biochim. Biophys. Acta* **2002**, *1595*, 131–144.
(2) Bridgman, P. W. *J. Biol. Chem.* **1914**, *19*, 511–512.
(3) Silva, J. L.; Weber, G. *Annu. Rev. Phys. Chem.* **1993**, *44*, 89–113.
(4) Heremans, K.; Smeller, L. *Biochim. Biophys. Acta* **1998**, *1386*, 353–370.
(5) Heremans, K. *Annu. Rev. Biophys. Bioeng.* **1982**, *11*, 1–21.
(6) Cooper, A. I. *J. Mater. Chem.* **2000**, *10*, 207–234.
(7) Kazarian, S. G. *Polym. Sci.* **2000**, *42*, 78–101.
(8) Tomasko, D. L.; Li, H.; Liu, D.; Han, X.; Wingert, M. J.; Lee, L. J.; Koelling, K. W. *Ind. Eng. Chem. Res.* **2003**, *42*, 6431–6456.
(9) Hofland, G. W.; de Rijke, A.; Thiering, R.; van der Wielen, L. A. M.; Witkamp, G. J. *J. Chromatogr., B: Biomed. Sci. Appl.* **2000**, *743*, 357–368.
(10) Thiering, R.; Hofland, G.; Foster, N.; Witkamp, G.-J.; van de Wielen, L. *Biotechnol. Prog.* **2001**, *17*, 513–521.
(11) Pasquali-Ronchetti, I.; Baccarani-Contri, M. *Microsc. Res. Tech.* **1997**, *38*, 428–435.
(12) Vrhovski, B.; Weiss, A. S. *Eur. J. Biochem.* **1998**, *258*, 1–18.
(13) Vrhovski, B.; Jensen, S.; Weiss, A. S. *Eur. J. Biochem.* **1997**, *250*, 92–98.
(14) Mithieux, S. M.; Weiss, A. S. *Adv. Protein Chem.* **2005**, *70*, 437–461.
(15) Mithieux, S. M.; Rasko, J. E. J.; Weiss, A. S. *Biomaterials* **2004**, *25*, 4921–4927.
(16) Leach Jennie, B.; Wolinsky Jesse, B.; Stone Phillip, J.; Wong Joyce, Y. *Acta Biomater.* **2005**, *1*, 155–164.
(17) Cox, B. A.; Starcher, B. C.; Urry, D. W. *Biochim. Biophys. Acta* **1973**, *317*, 209–213.
(18) Cox, B. A.; Starcher, B. C.; Urry, D. W. *J. Biol. Chem.* **1974**, *249*, 997–998.
(19) Kaibara, K.; Sakai, K.; Okamoto, K.; Uemura, Y.; Miyakawa, K.; Kondo, M. *Biopolymers* **1992**, *32*, 1173–1180.
(20) Kondo, M.; Nakashima, Y.; Kodama, H.; Okamoto, K. *J. Biochem.* **1987**, *101*, 89–94.
(21) Kazarian, S. G.; Chan, K. L. A. *Macromolecules* **2004**, *37*, 579–584.
(22) Fleming, O. S.; Chan, K. L. A.; Kazarian, S. G. *Polymer* **2006**, *47*, 4649–4658.
(23) Chan, K. L. A.; Kazarian, S. G. *Appl. Spectrosc.* **2003**, *57*, 381–389.
(24) Kazarian, S. G.; Chan, K. L. A. *Biochim. Biophys. Acta* **2006**, *1758*, 858–867.
(25) Burka, M. E.; Curbelo, R. US Patent No. 6141100, 2000.
(26) Sreerama, N.; Woody, R. W. *Anal. Biochem.* **2000**, *287*, 252–260.
(27) Partridge, S. M.; Davis, H. F. *Biochem. J.* **1955**, *61*, 21–30.
(28) Otake, K.; Shimomura, T.; Goto, T.; Imura, T.; Furuya, T.; Yoda, S.; Takebayashi, Y.; Sakai, H.; Abe, M. *Langmuir* **2006**, *22*, 4054–4059.
(29) Mammi, M.; Gotte, L.; Pezzin, G. *Nature* **1968**, *220*, 371–373.
(30) Debelle, L.; Alix, A. J. P.; Jacob, M.-P.; Huvenne, J.-P.; Berjot, M.; Sombret, B.; Legrand, P. *J. Biol. Chem.* **1995**, *270* (44), 26099–26103.
(31) Debelle, L.; Alix, A. J. P.; Wei, S. M.; Jacob, M.-P.; Huvenne, J.-P.; Berjot, M.; Legrand, P. *Eur. J. Biochem.* **1998**, *258* (2), 533–539.
(32) Debelle, L.; Alix, A. J. P. *J. Mol. Struct.* **1995**, *348*, 321–324.
(33) Schmidt, P.; Dybal, J.; Rodriguez-Cabello, J. C.; Reboto, V. *Biomacromolecules* **2005**, *6* (2), 697–706.
(34) Tamburro, A. M.; Guantieri, V.; Daga-Gordini, D.; Abatangelo, G. *Biochim. Biophys. Acta* **1977**, *492* (2), 370–376.
(35) Tamburro, A. M.; Guantieri, V.; Daga-Gordini, D.; Abatangelo, G. *J. Biol. Chem.* **1978**, *253* (9), 2893–2894.
(36) Urry, D. W.; Starcher, B.; Partridge, S. M. *Nature* **1969**, *222* (5195), 795–796.

BM700891B